Approximate Electrical Solution Of MHD Generator With Cathode Wall Nonuniformities

Author(s): C. C. P. Pian, A. W. Mcclaine, I. Sadovnik, and D.W. Swallom

Session Name: Channels II - Electrical Effects

SEAM: 21 (1983)

SEAM EDX URL: https://edx.netl.doe.gov/dataset/seam-21

EDX Paper ID: 1012

APPROXIMATE ELECTRICAL SOLUTION OF MHD GENERATOR WITH CATHODE WALL NONUNIFORMITIES*

C.C.P. Pian, A.W. McClaine, I. Sadovnik and D.W. Swallom

Avco Everett Research Laboratory, Inc.
Everett, Massachusetts 02149, U.S.A.

ABSTRACT

The effect of cathode wall nonuniformities on the electrical performance of Faraday loaded generators is modeled analytically. An approximate three-dimensional model is formulated to determine the distributions of the electrical variables within the MHD channel in the presence of cathode nonuniformities. Nonuniformities in this model are treated as a coarser resegmentation of the cathode wall. The electrical model is described and the calculated results are compared with experimental data.

INTRODUCTION

Cathode nonuniformities appear in MHD generators operating with slag-laden flows. These nonuniformities originate at the cathode wall when groups of electrodes are shorted by electrically polarized slag coatings.[1,2] The cause of the elevated slag conductivity is thought to be potassium or iron and iron oxide compounds driven into the cathode wall slag layer by the electric field within the channel.[3] The resulting change in the effective segmentation of the cathode wall causes a few insulator gaps to sustain the total Hall voltage of the generator. Normally, in the absence of cathode nonuniformities, this accumulated Hall voltage would divide approximately equally over all the cathode interelectrode gaps.

A typical interelectrode voltage distribution on the cathode wall of an Avco Mk VI channel is shown in Fig. 1. The particular data is obtained from an experiment using ash from a western U.S.A. coal. In the mid-channel region typically five to six cathode electrodes are electrically shorted. These shorted electrodes are separated by high voltage gaps which may be free of slag coating because of Joule dissipation from the Faraday current concentration at the downstream edge of the shorted group. Under similar experimental conditions but using eastern U.S.A. ash, the shorted groups involve typically three to four electrodes.[4]

The cathode nonuniformities are relatively steady. Over time the location of the high voltage gap may shift in the streamwise direction by one or more electrode pitches. Depending on the experimental conditions, the characteristic time of this phenomena is of the order of one to ten minutes.

These cathode wall nonuniformities can cause faults in diagonally loaded MHD generators (both diagonal conducting wall and diagonally connected) and drastically reduce the channel lifetimes. For this reason current control circuits are being developed for diagonally connected generators.[5] Cathode nonuniformities do not appear to be as destructive in segmented Faraday operation.[6] However, they do alter the electrical characteristics within the channel and may reduce the performance of the generator. In this paper, an approximate three-dimensional electrical model is formulated to study the effects of these cathode wall nonuniformities on

the internal electrical characteristics of Faraday generators. The electrical model has been incorporated into an MHD design and prediction computer code[7] in order to assess the effects of nonuniformities on overall generator performance.

The effects of cathode nonuniformities can be modeled by arbitrarily increasing the slag layer electrical conductivity to account for slag polarization. However, such an analytical approach can predict very large axial leakage currents which are not supported by experimental results.[4] The approach of this paper is to model the slag polarization/cathode nonuniformity effects as a change in the effective segmentation of the cathode wall.

APPROXIMATE FINITE-ELEMENT ELECTRICAL MODEL

An integral technique has been formulated to determine the distributions of the electrical variables within the MHD channel with a slag shorted cathode wall. Instead of solving Maxwell's equations exactly throughout the calculational domain, approximate solutions of the electrical variables are sought. These solutions are obtained from a closed set of equations which resulted from the description of the Faraday load connection and from the integration (averaging) of model electrical distributions across various finite regions. The finite element regions, as shown in Figs. 2 and 3, are formed by subdividing the calculational domain into various boundary layers, slag layers and core flow regions. The distributions of the electrical variables in these regions are determined such that the Ohm's law and certain additional electrical boundary conditions are satisfied.

In the electrode wall regions, a blending function approach[8] is used to prescribe the transverse variations of Hall field and Faraday current density. The lengths L_{EC} and L_{IC} define distances outward from the cathode electrode walls over which the E_x above the conducting segments and the J_y above the insulating segments build up to their respective "core" values. Corresponding anodic lengths are denoted by L_{EA} and L_{IA}. For example, above the cathode insulators,

$$J_{y_{IC}}(x,y) = J_{y_c}(x)\,\phi_{IC}(y) \tag{1}$$

and above the conductors,

$$E_{x_{EC}}(x,y) = E_{x_c}(x)\,\phi_{EC}(y) \tag{2}$$

The ϕ's are matching functions having the following properties:

$$\phi_{IC}(0) = \phi_{EC}(0) = 0 \tag{3a}$$

$$\phi_{IC}(L_{IC}) = \phi_{EC}(L_{EC}) = 1. \tag{3b}$$

Equation (3a) ensures that J_y vanishes on the surface of an insulator and E_x vanishes on the surface of a conductor. Equation (3b) ensures that J_y and E_x approach their core values at the edges of the electrical boundary layers. From periodicity and current conservation arguments, E_{xIC} and J_{yEC} can be approximated as:

$$E_{x_{IC}}(x,y) \cong E_{x_c}(x)\left\{1 + \frac{N(\ell_i + \ell_e) - \ell_i}{\ell_i}\left[1 - \phi_{EC}(y)\right]\right\} \tag{4}$$

and

$$J_{y_{EC}}(x,y) \cong J_{y_c}(x)\left\{1 + \frac{\ell_i}{N(\ell_i + \ell_e) - \ell_i}\left[1 - \phi_{IC}(y)\right]\right\} \tag{5}$$

where ℓ_e and ℓ_i refer to the conductor and insulator axial dimensions and N is the number of cathode conductor segments shorted by polarized slag. Similar expressions can be obtained for the anode wall regions by setting N equal to 1 and replacing subscripts IC by IA and EC by EA in the above equations. The remaining current densities and electric fields in the electrode wall regions are determined from the above model distributions and the Ohm's law, given the velocity, conductivity and Hall parameter distributions through the boundary layers. Proper values for the L's as functions of β, pitch-to-height ratio, boundary layer thickness, etc., are established from a two-dimensional electrical model.[9]

The sidewalls of the MHD generator are assumed to be electrically insulating so the core electric field can be imposed on the sidewall boundary layer regions:

$$E_{x_{SW}} = E_{x_c}(x) \tag{6}$$

and

$$E_{y_{SW}} = E_{y_c}(x). \tag{7}$$

The current densities can then be determined from Ohm's law and the gasdynamic and electrical parameters through the sidewall boundary layers:

$$J_{x_{SW}} = \frac{\sigma}{1+\beta^2}\left\{(1+\beta\,\beta_c)\,E_{x_c} - \frac{\beta(1+\beta_c^2)}{\sigma_c}\,J_{y_c} + \beta\sigma(u-u_c)B\right\} \tag{8}$$

and

$$J_{y_{SW}} = \frac{\sigma}{1+\beta^2}\left\{\frac{(1+\beta_c^2)}{\sigma_c}\,J_{y_c} + (\beta-\beta_c)\,E_{x_c} + (u-u_c)B\right\}. \tag{9}$$

The possibility of velocity overshoots in these boundary layers has also been taken into account.[6]

For the corner flow regions shown in Fig. 3, the following assumptions are made:

$$J_{y_{CRA}}(x,y,z) = J_{y_{SW}}(x,z)\,\phi_{IA}(y) \tag{10}$$

$$E_{x_{CRA}}(x,y) = E_{x_{IA}}(x,y) \tag{11}$$

$$J_{y_{CRC}}(x,y,z) = J_{y_{SW}}(x,z)\,\phi_{IC}(y) \tag{12}$$

and

$$E_{x_{CRC}}(x,y) = E_{x_{IC}}(x,y) \tag{13}$$

The current density assumptions preserve current conservation. The electric field assumptions are consistent with electrode wall and sidewall boundary layer fields. The variations of the remaining electrical variables in the corner regions are determined from Ohm's law.

The distributions of the electrical variables in the slag layers are determined from electrical conditions imposed from the boundary layer regions immediately above the slag layers. For the slag layers on electrode walls, values of axial electric field and transverse current density are imposed from the regions above. For the slag layers on the sidewalls, the axial and transverse fields are imposed. The remaining group of electrical variables are established from the slag layer Ohm's law.

The expressions for the electric fields and current densities can be integrated (averaged) in their respective regions given a suitable form of the blending functions, ϕ. The averaged value of electric fields and current densities obtained in this manner for the various regions have been listed in Appendix A for reference.

Several assumptions are made in the evaluation of the averaged axial current density in the corner flow regions. They are:

$$\langle \beta J_y \rangle_{CR} \cong \langle \beta \rangle_{CR} \langle J_y \rangle_{SW} \tag{14}$$

and

$$\langle \sigma E_x \rangle_{CR} \cong \langle \sigma \rangle_{CR} \langle E_x \rangle_{ele.\ wall} \tag{15}$$

where the corner averages of σ and β are computed as:

$$\langle f \rangle_{CR} \cong \frac{\langle f \rangle_{SW} \langle f \rangle_{ele.\ wall}}{f_{core}} \ . \tag{16}$$

Values of averaged slag conductivity are also assumed in the electrical model. Values of anode wall slag conductivity, $\langle \sigma \rangle_{SEW}$, and sidewall slag conductivity, $\langle \sigma \rangle_{SSW}$, are typically chosen to be from 0.2 mho/m to as high as 40 mho/m (Ref. 4) to represent conductivities of non-polarized slag. Current transport by means of concentrated arcs can be modeled by assuming the transverse slag conductivity, $\langle 1/\sigma \rangle_{SEW}$, equals zero, i.e., no transverse diffuse current. For situations where slag is completely burnt off from the high voltage cathode insulator gap, the cathode wall slag gap conductivity, $\langle \sigma \rangle_{SCW}$, equals zero. For cases where partial slag coverage remain over the cathode gap, a finite value of $\langle \sigma \rangle_{SCW}$ is assigned.

To solve the electrical components in the different finite regions, the loading conditions implied by the Faraday connection must now be imposed. These two Faraday conditions are: 1) the net axial current through a cross-sectional plane cutting through the electrode insulators (the plane depicted in Fig. 3) equals zero, and 2) the external voltage between the shorted cathode segment and an anode conductor must be equal to the sum of the internal voltage drops. The expressions resulting from the application of the loading conditions are listed in Appendix B. These two equations, along with the Ohm's law for the core flow region, form a closure for the core electrical solution. The electrical variables in all the other finite regions can be then determined once the core fields and current densities are known.

APPLICATION OF THE ELECTRICAL MODEL

The electrical model described in the previous section has been used to investigate the effects of cathode slag shorts on the local electrical characteristics in an Avco Mk VI generator. Results showing the sensitivities to model assumptions will now be discussed. The approximate electrical model has also been incorporated into a generator design and performance prediction code. Preliminary results of the performance prediction for a Mk VI generator will also be reported.

The sensitivity of the electrical solution to the length L_{EC} was investigated and the results for different assumed functional forms of characteristic lengths are shown in Fig. 4. The variation of the electrical variables in the core region is shown for different numbers of slag shorted cathodes. The results are obtained for the mid-channel conditions of the Mk VI generator. The solid lines are the results assuming L_{EC} is proportional to the "effective conductor length":

$$L_{EC} = k\,[N(\ell_e + \ell_i) - \ell_i] \tag{17}$$

and the dash lines are for results assuming:

$$L_{EC} = L_{EA} = k\,\ell_e. \tag{18}$$

The constant of proportionality, k, has been arbitrarily selected to be 0.15 in the present illustration. The strong dependence of the results on the assumed forms of L's indicate the importance of proper selections of the various characteristic lengths. This strong dependence motivated a two-dimensional investigation on the functional dependence of the characteristic lengths which is discussed in a separate paper.[9]

Results from the two-dimensional current stream function solver were used to estimate values for the characteristic lengths L_{EC}, L_{IC}, L_{EA} and L_{IA}. These lengths are determined by integrations of the two-dimensional electrical results and linear definitions of the blending functions ϕ_E and ϕ_I such that the integrals of the two-dimensional profiles equal the integrals of the linear distributions. Figure 5 shows the results of the present electrical model obtained by using those values of characteristic lengths that have been determined with the aid of the two-dimensional results. In the absence of cathode will nonuniformities (N = 1) and under the particular generator operating condition, there is practically no axial current at the mid-channel location of the generator. However, as the number of slag shorts increases, the flow of axial current in the generator also increases. The downstream flow of axial current is primarily through the core and sidewall boundary layer regions. The return path for this axial current is mainly through the cathode boundary layer region. The corresponding decrease in the magnitudes of the other electrical variables as the axial currents increase is also shown in Fig. 5.

The electrical conductivity of nonpolarized slag can vary significantly depending on the slag conditions and composition. The electrical model was used to investigate the effect of averaged slag conductivity [$\langle\sigma\rangle_{SEW}$ and $\langle\sigma\rangle_{SSW}$] on the local electrical characteristics of a Mk VI generator. The results are shown in Fig. 6 for both with (N = 5) and without (N = 1) cathode wall nonuniformity effects. Typically, the conductivity of unseeded nonpolarized slag is 0.2 to 4 mho/meter. As seed is absorbed, the values for nonpolarized slag can increase to 20 to 40 mho/m. The reduction in the slag layer impedance and the attendant increase in axial leakage current will lower the magnitudes of the other electrical variables, as can be seen in Fig. 6.

The finite-element electrical model has been incorporated into the AERL generator design and performance prediction code. Because of the nature of the electrical model, the generator performance degradations caused by cathode nonuniformities appear as segmentation losses. The results of the generator performance predictions for a Mk VI supersonic generator are shown in Table 1. With segmentation, agreement between analysis and data is relatively good without resorting to large electrode wall slag conductivities which are needed to achieve agreement using the infinite segmentation model. In both the finite and infinite segmentation analyses the power is predicted high and the Hall voltage low. Further work with the two dimensional model[9] should improve the finite segmentation results.

TABLE 1

COMPARISON OF DATA AND RESULTS USING THE INFINITE SEGMENTATION MODEL AND THE PRESENT FINITE SEGMENTATION MODEL

	DATA	Q3D Finite Segmentation	Infinite Segmentation
Mass Flow Rate (kg/s)	2.86	2.86	2.86
N/O	0.6	0.6	0.6
B (T)	2.9	2.9	2.9
Seed Flow Rate (percent)	1.0	1.0	1.0
Slag Conductivity (mho/m)	*	2.0	200.0
Electrical Power (kW)	315	350	354
Hall Voltage (kV)	1.780	1.67	1.66
Peak Electrode Current (A)	9.0	10.0	10.0
Peak Axial Electric Field (V/m)	1400	1400	1176
Total Channel Heat Loss (MW)	1.9	2.1	2.1

*Unmeasured

SUMMARY

An approximate three-dimensional electrical model has been developed for the purpose of predicting the effects of cathode wall nonuniformities on the internal electrical characteristics of Faraday generators. The cathode nonuniformities are treated in the model as a coarser resegmentation of the cathode electrodes. The electrical model is described in detail and some results showing the sensitivity to model assumptions are presented.

The computational time requirement of the electrical model is significantly lower than that for the more exact three-dimensional models.

The approximate electrical model has been incorporated into a generator design and performance prediction code. Comparisons were made between the predictions and experimental data from an Avco Mk VI generator run. Good agreements were obtained for both the integrated generator performance and the streamwise distributions of gasdynamic and elecrical variables. Further verifications with experimental data are in progress.

ACKNOWLEDGMENT

*This work supported by the U.S. Department of Energy under Contract No. DE-AC01-80ET15614.

REFERENCES

1. Petty, S.W., et al., "Electrode Phenomena in Slagging MHD Channels," 16th Symposium on Engineering Aspects of MHD, Pittsburgh (1977).

2. Demirjian, A.M., et al., "Electrode Development for Coal Fired MHD Generators," 17th Symposium on Engineering Aspects of MHD, Stanford (1978).

3. Koester, J.K. and Nelson, R.M., "Electrical Behavior of Slag Coatings in Coal-Fired MHD Generators," 16th Symposium on Engineering Aspects of MHD, Pittsburgh (1977).

4. Petty, S.W., "Effects of Cathode Slag Polarization on MHD Generator Performance," 8th International Conference on MHD Electrical Power Generation, Moscow, (1983).

5. Demirjian, A.M. and Quijano, I.M., "Power Conditioning and Control Requirements of Coal-Fired MHD Generators," Journal of Energy, Vol. 6 (1982).

6. Kessler, R., "MHD Generator Channel Design," Specialists Meeting on Coal Fired MHD Power Generation, Sydney (1981).

7. Gertz, J., et al., "Modeling of MHD Channel Boundary Layers Using an Integral Approach," 18th Symposium on Engineering Aspects of MHD, Butte (1979).

8. Oliver, D.A., "The Prediction of Inter-Electrode Breakdown in MHD Generators," 14th Symposium on Engineering Aspects of MHD, Tullahoma (1974).

9. Pian, C.C.P., Sadovnik, I. and McClaine, A.W., "Analytical Investigations of the Effects of Cathode Nonuniformities on MHD Generator Characteristics," 8th International Conference on MHD Electrical Power Generation, Moscow, USSR, (1983).

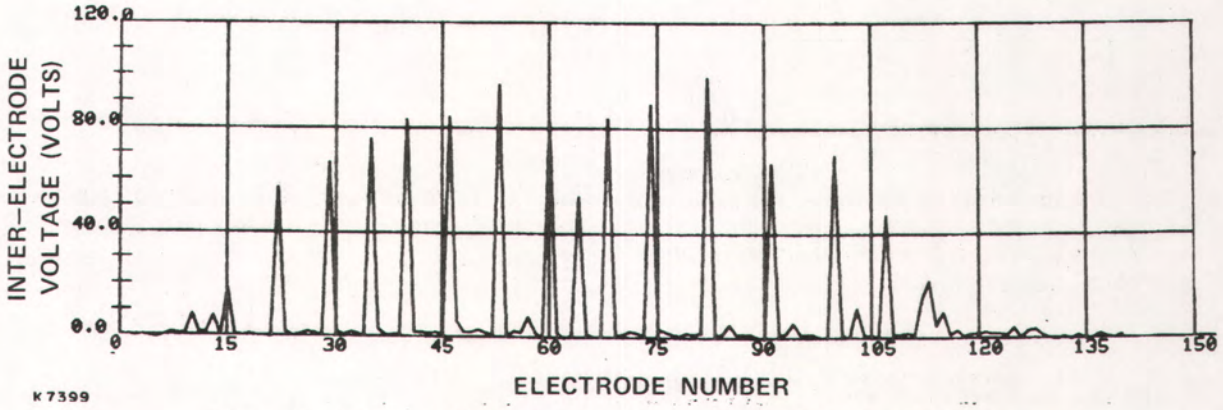

Fig. 1 Voltage Distribution on Cathode Wall in the Presence of Slag Nonuniformities

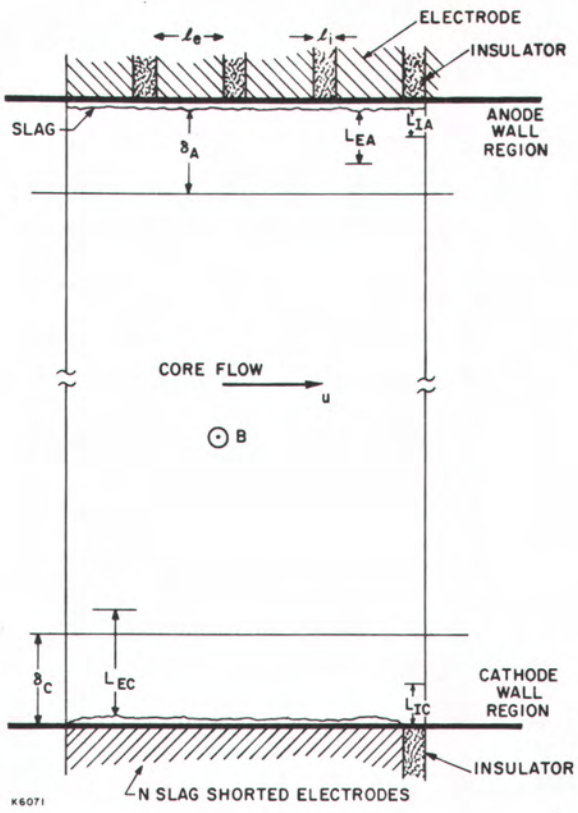

Fig. 2 Regions of the Three-Dimensional Electrical Model

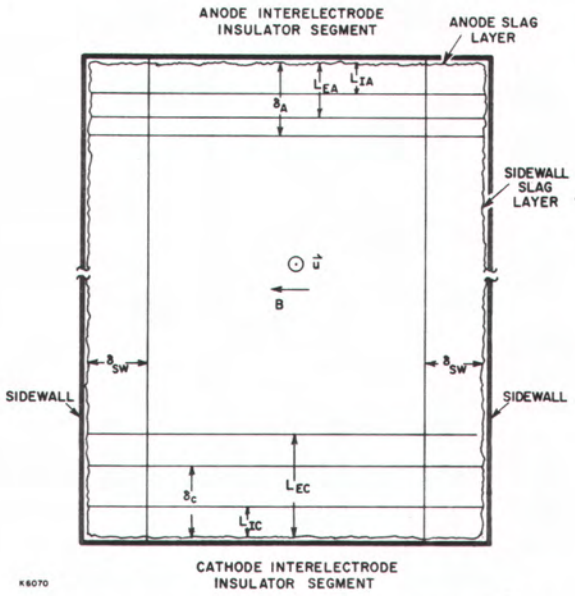

Fig. 3 Cross Plane through the Inter-electrode Insulator

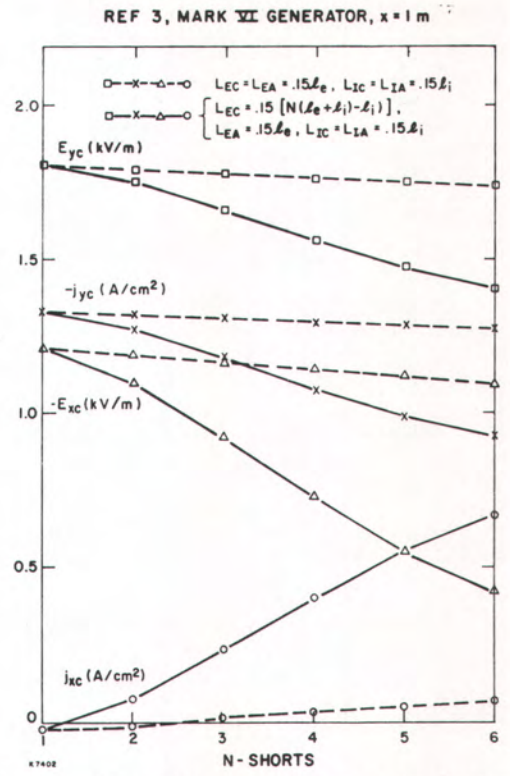

Fig. 4 Core Values of Electrical Variables vs Number of Cathode Slag Shorts

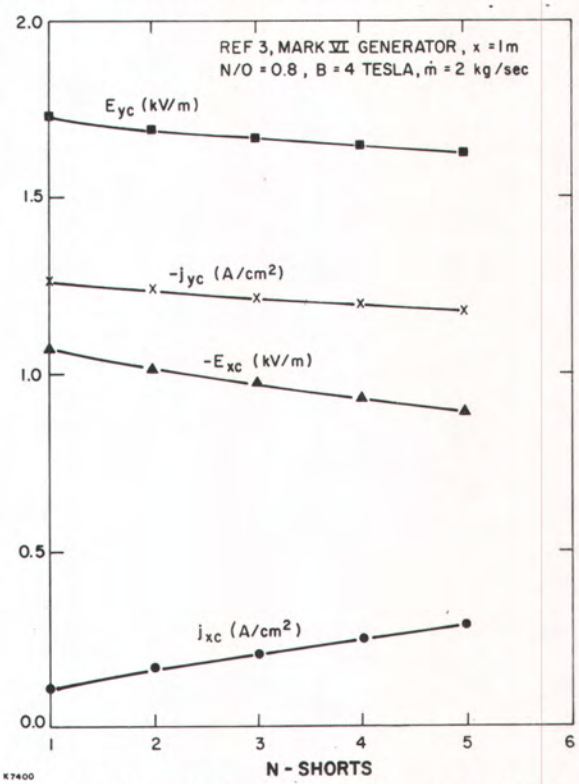

Fig. 5 Core Values of Electrical Variables vs Number of Cathode Electrodes in Slag Shorted Group

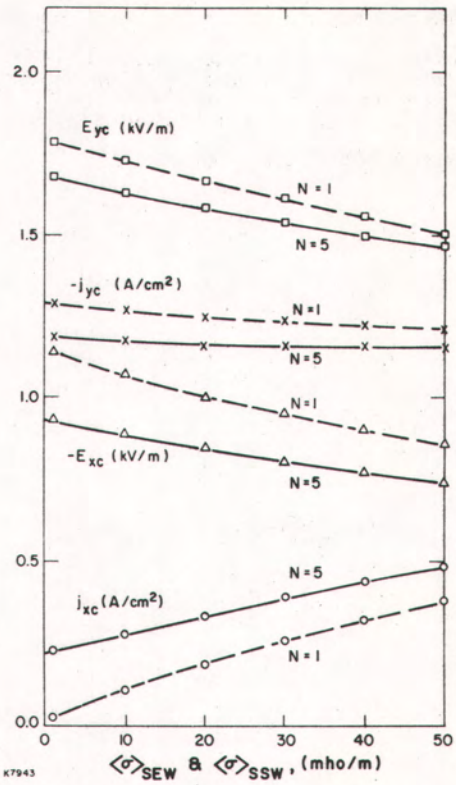

Fig. 6 Variations of Generator Electrical Characteristics as a Function of Averaged Anode and Sidewall Slag Conductivities

APPENDIX A

The expressions for the averaged Faraday fields and averaged Hall current densities in the various regions shown in Figures A1 and A2 are listed in this appendix.

Cathode Wall Regions

Region C1:

$$\langle E_y\rangle_{C1} = E_{xc}\left\{\langle\beta\phi_{EC}\rangle_{C1}\left[N\left(1+\frac{\ell_e}{\ell_i}\right)-1\right]-\langle\beta\rangle_{C1}\,N\left(1+\frac{\ell_e}{\ell_i}\right)\right\}$$

$$+\left\langle\frac{1+\beta^2}{\sigma}\phi_{IC}\right\rangle_{C1} J_{yc}+\langle U\rangle_{C1}\,B \qquad \text{(A1)}$$

$$\langle J_x\rangle_{C1} = E_{xc}\left\{\langle\sigma\phi_{EC}\rangle_{C1}+N\left(1+\frac{\ell_e}{\ell_i}\right)\left(\langle\sigma\rangle_{C1}-\langle\sigma\phi_{EC}\rangle_{C1}\right)\right\}$$

$$-\langle\beta\phi_{IC}\rangle_{C1}\,J_{yc} \qquad \text{(A2)}$$

where

$$\langle f\rangle_{C1} \equiv \frac{1}{L_{IC}}\int_0^{L_{IC}} f(y)\,dy \qquad \text{(A3)}$$

Region C2:

$$\langle E_y\rangle_{C2} = E_{xc}\left\{\langle\beta\phi_{EC}\rangle_{C2}\left[N\left(1+\frac{\ell_e}{\ell_i}\right)-1\right]-\langle\beta\rangle_{C2}\,N\left(1+\frac{\ell_e}{\ell_i}\right)\right\}$$

$$+J_{yc}\left\langle\frac{1+\beta^2}{\sigma}\right\rangle_{C2}+\langle U\rangle_{C2}\,B \qquad \text{(A4)}$$

$$\langle J_x\rangle_{C2} = E_{xc}\left\{\langle\sigma\phi_{EC}\rangle_{C2}+N\left(1+\frac{\ell_e}{\ell_i}\right)\left(\langle\sigma\rangle_{C2}-\langle\sigma\phi_{EC}\rangle_{C2}\right)\right\}$$

$$-\langle\beta\rangle_{C2}\,J_{yc} \qquad \text{(A5)}$$

where

$$\langle f\rangle_{C2} \equiv \frac{1}{\delta_c - L_{IC}}\int_{L_{IC}}^{\delta_c} f(y)\,dy \qquad \text{if } \delta_c < L_{EC}$$

$$\equiv \frac{1}{L_{EC}-L_{IC}}\int_{L_{IC}}^{L_{EC}} f(y)\,dy \qquad \text{if } \delta_c > L_{EC} \qquad \text{(A6)}$$

Region C3:

$$\langle E_y\rangle_{C3} = \beta_c E_{xc}\left\{\langle\phi_{EC}\rangle_{C3}\left[N\left(1+\frac{\ell_e}{\ell_i}\right)-1\right]-N\left(1+\frac{\ell_e}{\ell_i}\right)\right\}$$

$$+\frac{1+\beta_c^2}{\sigma_c}J_{yc}+U_c B \qquad \text{if } \delta_c < L_{EC}$$

$$=-\langle\beta\rangle_{C3}E_{xc}+\left\langle\frac{1+\beta^2}{\sigma}\right\rangle_{C3}J_{yc} \qquad \text{(A7)}$$

$$+\langle U\rangle_{C3}\,B \qquad \text{if } \delta_c > L_{EC}$$

$$\langle J_x\rangle_{C3} = \sigma_c E_{xc}\left\{\langle\phi_{EC}\rangle_{C3}+N\left(1+\frac{\ell_e}{\ell_i}\right)\left(1-\langle\phi_{EC}\rangle_{C3}\right)\right\}$$

$$-\beta_c J_{yc} \qquad \text{if } \delta_c < L_{EC}$$

$$=\langle\sigma\rangle_{C3}E_{xc}-\langle\beta\rangle_{C3}J_{yc} \qquad \text{if } \delta_c > L_{EC} \qquad \text{(A8)}$$

where

$$\langle f\rangle_{C3} \equiv \frac{1}{L_{EC}-\delta_c}\int_{\delta_c}^{L_{EC}} f(y)\,dy \qquad \text{if } \delta_c < L_{EC}$$

$$\equiv \frac{1}{\delta_c - L_{EC}}\int_{L_{EC}}^{\delta_c} f(y)\,dy \qquad \text{if } \delta_c > L_{EC} \qquad \text{(A9)}$$

Region C4:

$$\langle E_y \rangle_{C4} = J_{yc} \left[\left\langle \frac{1+\beta^2}{\sigma} \right\rangle_{C4} N\left(1 + \frac{\ell_e}{\ell_i}\right) - \left\langle \frac{1+\beta^2}{\sigma} \phi_{IC} \right\rangle_{C4} \right] \left[N\left(1 + \frac{\ell_e}{\ell_i}\right) - 1 \right]^{-1} - \langle \beta \phi_{EC} \rangle_{C4} E_{xc} + \langle U \rangle_{C4} B \quad \text{(A10)}$$

$$\langle J_x \rangle_{C4} = - J_{yc} \left[\langle \beta \rangle_{C4} N\left(1 + \frac{\ell_e}{\ell_i}\right) - \langle \beta \phi_{IC} \rangle_{C4} \right] \left[N\left(1 + \frac{\ell_e}{\ell_i}\right) - 1 \right]^{-1} + \langle \sigma \phi_{EC} \rangle_{C4} E_{xc} \quad \text{(A11)}$$

where

$$\langle f \rangle_{C4} = \langle f \rangle_{C1} \quad \text{(A12)}$$

Region C5:

$$\langle E_y \rangle_{C5} = \left\langle \frac{1+\beta^2}{\sigma} \right\rangle_{C5} J_{yc} - \langle \beta \phi_{EC} \rangle_{C5} E_{xc} + \langle U \rangle_{C5} B \quad \text{(A13)}$$

$$\langle J_x \rangle_{C5} = \langle \sigma \phi_{EC} \rangle_{C5} E_{xc} - \langle \beta \rangle_{C5} J_{yc} \quad \text{(A14)}$$

where

$$\langle f \rangle_{C5} = \langle f \rangle_{C2} \quad \text{(A15)}$$

Region C6:

$$\langle E_y \rangle_{C6} = \frac{1+\beta_c^2}{\sigma_c} J_{yc} - \beta_c \langle \phi_{EC} \rangle_{C6} E_{xc} + U_c B \qquad \text{if } \delta_C < L_{EC}$$

$$= \left\langle \frac{1+\beta^2}{\sigma} \right\rangle_{C6} J_{yc} - \langle \beta \rangle_{C6} E_{xc} + \langle U \rangle_{C6} B \qquad \text{if } \delta_C > L_{EC} \quad \text{(A16)}$$

$$\langle J_x \rangle_{C6} = \sigma_c \langle \phi_{EC} \rangle_{C6} E_{xc} - \beta_c J_{yc} \qquad \text{if } \delta_C < L_{EC} \quad \text{(A17)}$$

$$= \langle \sigma \rangle_{C6} E_{xc} - \langle \beta \rangle_{C6} J_{yc} \qquad \text{if } \delta_C > L_{EC}$$

where

$$\langle f \rangle_{C6} = \langle f \rangle_{C3} \quad \text{(A18)}$$

Anode Wall Regions

Expressions for the averaged electric fields and current densities in regions A1 to A6 can be obtained from the corresponding cathode wall expressions after setting N to 1 and replacing subscripts IC by IA and EC by EA.

Sidewall Boundary Layer Regions

$$\langle E_y \rangle_{SW} = \frac{1+\beta_c^2}{\sigma_c} J_{yc} - \beta_c E_{xc} + U_c B \quad \text{(A19)}$$

$$\langle J_x \rangle_{SW} = E_{xc} \left[\left\langle \frac{\sigma}{1+\beta^2} \right\rangle_{SW} + \beta_c \left\langle \frac{\beta\sigma}{1+\beta^2} \right\rangle_{SW} \right] - \left\langle \frac{\beta\sigma}{1+\beta^2} \right\rangle_{SW} \frac{1+\beta^2}{\sigma_c} J_{yc} + B \left[\left\langle \frac{Bu\sigma}{1+\beta^2} \right\rangle_{SW} - U_c \left\langle \frac{\beta\sigma}{1+\beta^2} \right\rangle_{SW} \right] \quad \text{(A20)}$$

where

$$\langle f \rangle_{SW} \equiv \delta_{SW}^{-1} \int_0^{\delta_{SW}} f(z)\, dz \quad \text{(A21)}$$

Corner Flow Regions

Region CRC1:

$$\langle J_x \rangle_{CRC1} \simeq \langle \sigma \rangle_{CRC1} \langle E_x \rangle_{C1} - \langle \beta \rangle_{CRC1} \langle J_y \rangle_{SW} \langle \phi_{IC} \rangle_{C1} \quad \text{(A22)}$$

where

$$\langle f \rangle_{CRC1} \simeq \langle f \rangle_{CRC2} \langle f \rangle_{C1} f_c^{-1} \quad \text{(A23)}$$

Region CRC2:

$$\langle J_x \rangle_{CRC2} \simeq \langle \sigma \rangle_{CRC2} \langle E_x \rangle_{C2} - \langle \beta \rangle_{CRC2} \langle J_y \rangle_{SW} \quad \text{(A24)}$$

where

$$\langle f \rangle_{CRC2} \simeq \langle f \rangle_{CRC3} \langle f \rangle_{C2} f_c^{-1} \quad \text{(A25)}$$

Region CRC3:

$$\langle J_x \rangle_{CRC3} \simeq \langle \sigma \rangle_{CRC3} \langle E_x \rangle_{C3} - \langle \beta \rangle_{CRC3} \langle J_y \rangle_{SW} \quad \text{(A26)}$$

where

$$\langle f \rangle_{CRC3} \simeq \langle f \rangle_{SW} \langle f \rangle_{C3} f_c^{-1} \quad \text{(A27)}$$

Expressions for the averaged electrical variables in regions CRA1 - CRA3 can be obtained from the corresponding cathode corner expressions with appropriate changes in the subscripts.

Slag Layer Regions

Region SC1:

$$\langle J_x \rangle_{SC1} = \langle \sigma \rangle_{SCW} N(1 + \frac{\ell_e}{\ell_i}) E_{xc} \qquad (A28)$$

Region SC2:

$$\langle E_y \rangle_{SC2} = \langle \frac{1}{\sigma} \rangle_{SEW} N(1 + \frac{\ell_e}{\ell_i}) J_{yc} \qquad (A29)$$

Analogous expressions apply to regions SA1 and SA2.

Region SCSC:

$$\langle J_x \rangle_{SCSC} = \langle \sigma \rangle_{SSW} \langle E_x \rangle_{CRC} \qquad (A30)$$

Region CCSC:

$$\langle J_x \rangle_{CCSC} = \langle \sigma \rangle_{SEW} \langle E_x \rangle_{CRC1} \qquad (A31)$$

Similar expressions apply to regions SASC and AASC.

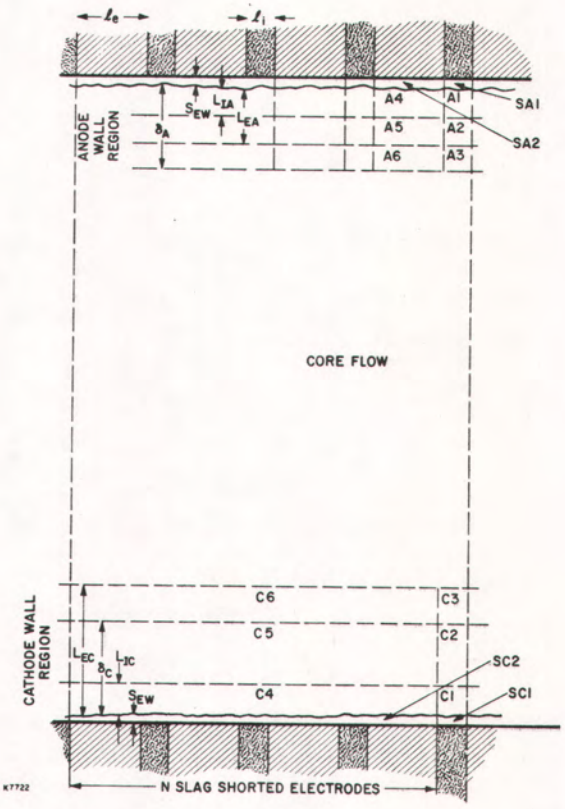

Fig. A1 Labeling of the Various Divisions in the Electrode Wall Regions

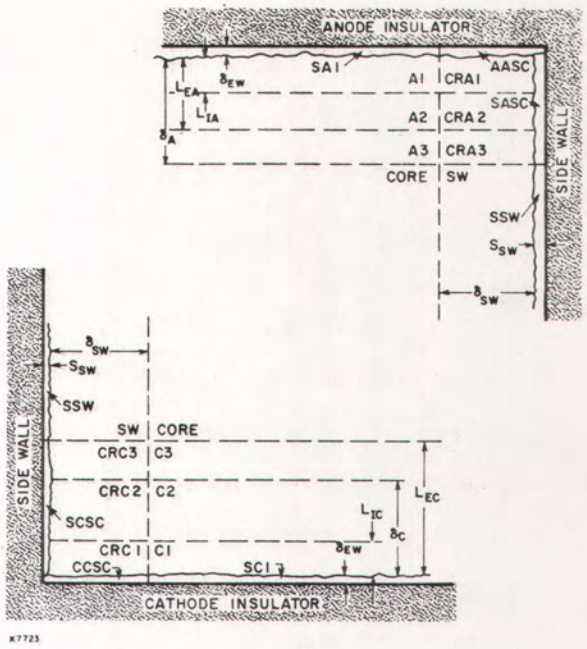

Fig. A2 Labeling of the Various Sub-Divisions in the Corner Regions

APPENDIX B

Faraday Connection:

$$V_{arc} + K_{ext} U_c BH = E_{yc} H_c + \langle E_y \rangle_{SC2} H_{SC2} + \langle E_y \rangle_{C4} H_{C4} + \langle E_y \rangle_{C5} H_{C5} + \langle E_y \rangle_{C6} H_{C6} + \langle E_y \rangle_{A6} H_{A6} + \langle E_y \rangle_{A5} H_{A5} + \langle E_y \rangle_{A4} H_{A4} + \langle E_y \rangle_{SA2} H_{SA2} \qquad (B1)$$

where

$$H_c = H - \delta_A - L_{EC} - 2S_{EW}$$

$$H_{SC2} = S_{EW}$$

$$H_{C4} = L_{IC}$$

$$H_{C5} = \delta_C - L_{IC} \quad \text{if } \delta_C < L_{EC}$$

$$= L_{EC} - L_{IC} \quad \text{if } \delta_C > L_{EC}$$

$$H_{C6} = L_{EC} - \delta_C \quad \text{if } \delta_C < L_{EC}$$

$$= \delta_C - L_{EC} \quad \text{if } \delta_C > L_{EC}$$

$$H_{A6} = \delta_A - L_{EA}$$

$H_{A5} = L_{EA} - L_{IA}$

$H_{A4} = L_{IA}$

$H_{SA2} = S_{EW}$

V_{arc} = Arc Voltage Drop

K_{ext} = Load Factor

Current Equation:

$$I_H = J_{xc}A_c + 2\langle J_x\rangle_{SW} A_{SW} + 2\langle J_x\rangle_{SSW} A_{SSW} + \langle J_x\rangle_{A1} A_{A1}$$
$$+ \langle J_x\rangle_{A2} A_{A2} + \langle J_x\rangle_{A3} A_{A3} + \langle J_x\rangle_{SA1} A_{SA1} + 2\langle J_x\rangle_{CRA3} A_{CRA3}$$
$$+ 2\langle J_x\rangle_{CRA2} A_{CRA2} + 2\langle J_x\rangle_{CRA1} A_{CRA1} + \langle J_x\rangle_{C3} A_{C3}$$
$$+ \langle J_x\rangle_{C2} A_{C2} + \langle J_x\rangle_{C1} A_{C1} + 2\langle J_x\rangle_{CRC3} A_{CRC3}$$
$$+ 2\langle J_x\rangle_{CRC2} A_{CRC2} + 2\langle J_x\rangle_{CRC1} A_{CRC1}$$
$$+ \langle J_x\rangle_{SC1} A_{SC1} + 2\langle J_x\rangle_{SCSC} A_{SCSC}$$
$$+ 2\langle J_x\rangle_{SASC} A_{SASC} + 2\langle J_x\rangle_{CCSC} A_{CCSC}$$
$$+ 2\langle J_x\rangle_{AASC} A_{AASC} \qquad (B2)$$

where

$A_c = H_c D_c$

$D_c = D - 2\delta_{SW} - 2\delta_{SW}$

$A_{SW} = H_c \delta_{SW}$

$A_{SSW} = H_c S_{SW}$

$A_{A1} = D_c L_{IA}$

$A_{A2} = D_c (L_{EA} - L_{IA})$

$A_{A3} = D_c (\delta_A - L_{EA})$

$A_{SA1} = D_c S_{EW}$

$A_{CRA3} = \delta_{SW} (\delta_A - L_{EA})$

$A_{CRA2} = \delta_{SW} (L_{EA} - L_{IA})$

$A_{CRA1} = \delta_{SW} L_{IA}$

$A_{C3} = D_c (L_{EC} - \delta_C)$ if $\delta_C < L_{EC}$

$= D_c (\delta_C - L_{EC})$ if $\delta_C > L_{EC}$

$A_{C2} = D_c (\delta_C - L_{IC})$ if $\delta_C < L_{EC}$

$= D_c (L_{EC} - L_{IC})$ if $\delta_C > L_{EC}$

$A_{C1} = D_c L_{IC}$

$A_{CRC3} = \delta_{SW} (L_{EC} - \delta_C)$ if $\delta_C < L_{EC}$

$= \delta_{SW} (\delta_C - L_{EC})$ if $\delta_C > L_{EC}$

$A_{CRC2} = \delta_{SW} (\delta_C - L_{IC})$ if $\delta_C < L_{EC}$

$= \delta_{SW} (L_{EC} - L_{IC})$ if $\delta_C > L_{EC}$

$A_{CRC1} = \delta_{SW} L_{IC}$

$A_{SC1} = D_c S_{EW}$

$A_{SCSC} = L_{EC} S_{SW}$ if $\delta_C < L_{EC}$

$= \delta_C S_{SW}$ if $\delta_C > L_{EC}$

$A_{SASC} = \delta_A S_{SW}$

$A_{CCSC} = S_{EW} [S_{SW} + \delta_{SW}]$

$A_{AASC} = S_{EW} [S_{SW} + \delta_{SW}]$

I_H = Leakage Hall Current